

Complete temporal characterization of a single photon

Zhongzhong Qin,^{1,2} Adarsh S. Prasad,¹ Travis Brannan,¹ Andrew MacRae,³ A. Lezama,⁴ and A. I. Lvovsky^{1,5,*}

¹*Institute for Quantum Science and Technology,
University of Calgary, Alberta T2N1N4, Canada*

²*Quantum Institute for Light and Atoms, State Key Laboratory of Precision Spectroscopy,
East China Normal University, Shanghai 200062, People's Republic of China*

³*Department of Physics, University of California, Berkeley, California 94720, USA*

⁴*Instituto de Física, Facultad de Ingeniería, Universidad de la República,
J. Herrera y Reissig 565, Montevideo 11300, Uruguay*

⁵*Russian Quantum Centre, 100 Novaya St., Skolkovo, Moscow 143025, Moscow, Russia*

(Dated: June 12, 2022)

Abstract

Precise information about the temporal mode of optical states is crucial for optimizing their interaction efficiency between themselves and/or with matter in various quantum communication devices. Here we propose and experimentally demonstrate a method of determining both the real and imaginary components of a single photon's temporal density matrix by measuring the autocorrelation function of the photocurrent from a balanced homodyne detector at multiple local oscillator frequencies. We test our method on single photons heralded from biphotons generated via four-wave mixing in an atomic vapor and obtain excellent agreement with theoretical predictions for several settings.

Introduction

Single photons and single photon qubits are among the foundations of most quantum optical information processing techniques such as cryptography [1], teleportation [2], repeaters [3] and computing [4]. Many of these applications require the photons to have a well-defined, pure modal structure. Possessing precise information about that structure is essential for quantum-optical technology.

An approximate guess of a photon's mode can be inferred theoretically from the characteristics of the source [5–9], but this information is not always available or reliable. For example, this approach would not work for photons sent in by a remote party in a communication scheme, or for photons from an incompletely characterized mesoscopic source. Therefore, it is important to have a technique for precise characterization of a photon's mode experimentally. While such techniques are relatively well developed for spatial modes [10, 11], their extension into the temporal domain is challenging.

One approach to studying the temporal structure of the photon would be to look at the photon detection event statistics as a function of time. For example, this approach has been used to study the timing of coherent double Raman scattering from an atomic ensemble [12]. Further insight into the photon preparation quality can be gained by studying time-dependent photon counting autocorrelation statistics [13]. However, these techniques provide no information about the phase coherence between different segments of the photon's temporal mode.

Complete information about a photon's temporal properties can be obtained by studying its interference with a classical field. Polycarpou *et al.* used adaptive waveform shaping of local oscillator (LO) pulses [14] to heuristically find the LO temporal mode that maximizes the

efficiency of homodyne detection of the photon. This occurs when the LO temporal mode matches that of the signal, enabling measurement of that mode. However, physical shaping of LO pulses is quite sophisticated experimentally. Furthermore, this technique has only been demonstrated for pure temporal modes.

For a photon with bandwidth resolvable by detection electronics, the time domain statistics may be measured directly and in real time by analyzing the time-dependent statistics of the homodyne detector's output photocurrent with a continuous-wave LO. MacRae *et al.* [15, 16] showed that the autocorrelation function of this photocurrent estimates the real part of the density matrix defining the photon's temporal mode. Subsequently, this approach has been utilized for the “Schrödinger cat” and two-photon Fock states [17].

However, this method does not yield any information about the imaginary part of the photon's temporal density matrix (TDM). In this paper we present an experimental technique of *polychromatic optical heterodyne tomography*, which relies on acquiring the autocorrelation data of the homodyne photocurrent at multiple LO frequencies. The method enables us to determine both the real and imaginary parts of the photon's TDM, or, equivalently, both its amplitude and phase, thereby completely characterizing its temporal state. It works equally well for pure and mixed temporal modes.

Methods

The (pure) temporal mode of a photon is defined by annihilation operator

$$\hat{A}_\phi = \int_{-\infty}^{\infty} \hat{a}_t \phi(t) dt, \quad (1)$$

where $\phi(t)$ is the temporal mode function (TMF) and \hat{a}_t represents the instantaneous annihilation operator at

time t [18]. A single photon state in this mode is then given by $|1_\phi\rangle = \hat{A}_\phi^\dagger |0\rangle = \int_{-\infty}^{\infty} \phi^*(t) |1_t\rangle dt$, where $|1_t\rangle = \hat{a}_t^\dagger |0\rangle$.

The digital nature of the data acquisition system used in our experiment compels us to represent the temporal modes in terms of discrete time bins. The single photon state in temporal mode $\phi(t)$ can then be approximately expressed as $|1_\phi\rangle = \sum_j \phi^*(t_j) |1_j\rangle$ with $\sum_j |\phi(t_j)|^2 = 1$. Here t_j is the time associated with the j^{th} bin and $|1_j\rangle$ is the state containing one photon in the top-hat temporal mode associated with the j^{th} bin and vacuum in all other bins. The density operator of the photon is then represented as $\sum_{mn} \rho_{mn} |1_m\rangle \langle 1_n|$ where ρ_{mn} is the temporal density matrix.

The homodyne current for the j^{th} time bin $I(t_j)$ is proportional to the quadrature

$$\hat{X}_j = (\hat{a}_j e^{-i\theta_j} + \hat{a}_j^\dagger e^{i\theta_j}) / \sqrt{2}, \quad (2)$$

where $\theta_j = \delta\omega \cdot t_j + \theta_0$ is the optical phase difference between the LO and the signal. Here $\delta\omega$ is the frequency detuning between the LO and the signal and θ_0 the LO relative phase at $t = 0$. The autocorrelation matrix for the homodyne current is then

$$\begin{aligned} \langle I(t_j) I(t_k) \rangle &\propto \langle \hat{X}_j \hat{X}_k \rangle = \text{Tr}[\hat{\rho} \hat{X}_j \hat{X}_k] \\ &= \sum_{mn} \rho_{mn} \langle 1_n | \hat{X}_j \hat{X}_k | 1_m \rangle, \end{aligned} \quad (3)$$

where each matrix element can be evaluated using Eq. (2) as

$$\begin{aligned} \langle 1_n | \hat{X}_j \hat{X}_k | 1_m \rangle & \quad (4) \\ &= \frac{1}{2} \left[e^{-i\delta\omega(t_k - t_j)} \delta_{km} \delta_{nj} + \delta_{jk} \delta_{nm} + e^{-i\delta\omega(t_j - t_k)} \delta_{jm} \delta_{nk} \right]. \end{aligned}$$

Note that Eq. (4) does not depend on θ_0 due to the phase uncertainty of Fock states.

From Eqs. (3) and (4), one can obtain

$$\langle \hat{X}_j \hat{X}_k \rangle = \frac{1}{2} \delta_{jk} + A_{jk}. \quad (5)$$

The first term in Eq. (5) corresponds to the autocorrelation matrix for the vacuum. The second term, which we call the *reduced* autocorrelation matrix, is directly related to the photon's TDM:

$$A_{jk} = \text{Re}[\rho_{jk}] \cos[\delta\omega(t_j - t_k)] + \text{Im}[\rho_{jk}] \sin[\delta\omega(t_j - t_k)]. \quad (6)$$

If the LO frequency is same as that of the signal, i.e., at $\delta\omega = 0$, the autocorrelation matrix depends only on the real part of the TDM. However, by using $\delta\omega \neq 0$ one obtains access to its imaginary part.

In a realistic experiment, the photon being tested may experience losses, resulting in admixture of the vacuum

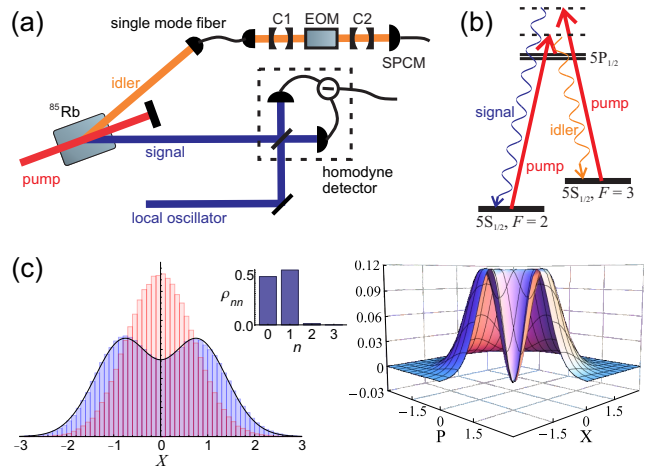


FIG. 1. (a) Schematic of the experimental set-up (C1, C2: filter cavities; EOM: electro-optic modulator; SPCM: single photon counting module). The signal (blue) goes to the homodyne detector, whereas the idler (orange) passes through C1 (55 MHz) and C2 (7 MHz) before detection via the SPCM. The EOM between C1 and C2 is optional. (b) The ^{85}Rb three-level Λ system, with the fields' configuration shown. (c) Reconstruction of the state of the electromagnetic field in the temporal mode determined experimentally (unmodulated case). Left to right: experimental quadrature distribution (blue) overlaid with that for the vacuum state (red); diagonal elements of the Fock-basis density matrix; Wigner function. The single-photon fraction is 52.9%.

into the state detected. Our technique would still apply to this case, but the second term would enter Eq. (5) with the coefficient equal to the transmissivity of the lossy element. For high losses, acquisition of larger quantities of data may be necessary to reduce the statistical uncertainties [22].

Our experimental scheme for creating the single-photon state and measuring the autocorrelation matrix is shown in Fig. 1. We use coherent double Raman scattering (four-wave mixing) in an ensemble of Λ -type atoms to generate a two-mode squeezed state in a non-degenerate phase-matched configuration [16]. A hot ^{85}Rb vapor cell is pumped by a 1 Watt laser beam at 795 nm derived from a continuous-wave Ti:Sapphire laser. The signal and idler beams are spatially separated from the pump, and a specific spatial mode is selected in the idler channel using a single-mode fiber. Subsequently, the idler channel is subjected to spectral filtering by means of a lens cavity (C1) of a 55 MHz bandwidth [19] and a conventional Fabry-Perot cavity (C2) of bandwidth $\gamma/2\pi = 7$ MHz. The usage of two cavities with incommensurate free spectral ranges ensures that the combined spectral filter has a single transmission peak of 7 MHz width. This results in a heralded photon with a temporal mode that can be easily resolved by our homodyne detector with a 100 MHz bandwidth [20].

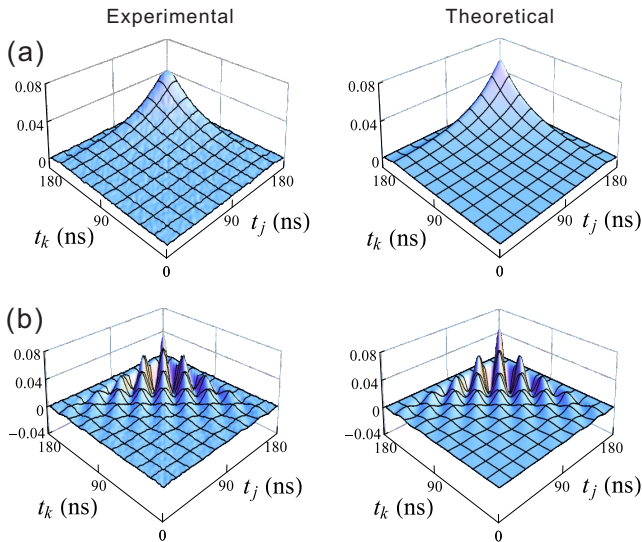


FIG. 2. Theoretical (right) and experimental (left) reduced autocorrelation matrices, for two different LO detunings: (a) 0 MHz and (b) 27 MHz, corresponding to the measurement setting without modulation. The trigger photon arrives at $t = 155$ ns.

The idler beam is then coupled to a PerkinElmer single photon counting module (SPCM) with a dark count rate below 100 Hz. Both cavities are maintained at a stable frequency by using an alignment beam which is unblocked every few seconds to monitor and readjust the cavity resonance frequency. Detection of an idler photon projects the signal onto a single photon in a well-defined spatio-temporal mode conjugate to the idler. This signal channel is mode-matched with a continuous-wave LO (18 mW) for homodyne detection [20]. The LO is derived from a diode laser that is locked and phase stabilized with respect to the pump using an optical phase-lock loop [21].

A click from the SPCM in the idler channel acts as the trigger for the measurement of the signal. The homodyne photocurrent is recorded for 360 ns around the trigger point as reference with a time binning of 2 ns. For each LO detuning, the autocorrelation matrix (3) of the homodyne photocurrent is obtained by taking an average over 2 million traces.

Theoretically, the data corresponding to two LO detunings would constitute a quorum for the temporal mode reconstruction. Experimentally, however, we take data at eight different detunings to avoid the situation where the sinusoids in Eq. (6) approach zero for all detunings simultaneously and to enhance the statistical accuracy of the recovered $\hat{\rho}$.

Once the autocorrelation matrices have been acquired, we process them to eliminate the vacuum term in Eq. (5), as well as any contributions from the DC bias in the homodyne photocurrent and thermal background. These contributions are not correlated with trigger events, and

are only dependent on the difference $t_j - t_k$. They can therefore be evaluated as the mean autocorrelation value along lines $t_j - t_k = \text{const}$ for the data points acquired significantly after the trigger pulse where no signal photon is expected. Subtracting them from the autocorrelation matrix yields the reduced autocorrelation matrix (Fig. 2) [22].

The TDM can now be determined by solving Eq. (6) for each pair (j, k) . However, such direct approach does not ensure positivity and normalization of the reconstructed density operator. To incorporate these *a priori* constraints into the reconstruction, we implement a more sophisticated iterative optimization algorithm. The algorithm uses the eight experimental reduced autocorrelation matrices as the training set. The difference between the experimental left-hand side of Eq. (6) and the right-hand side of that equation evaluated from the estimated TDM, squared and summed over all pairs (j, k) and all LO frequencies, is used as the cost function. Iterations utilize the diagonal representation of the TDM: $\hat{\rho} = \sum_i p_i |\psi_i\rangle \langle \psi_i|$. In the first step of each iteration, the eigenvalues p_i are adjusted to minimize the cost function while keeping them real, non-negative and totalling 1. In the second step, the eigenvectors $|\psi_i\rangle$ are optimized by pairwise unitary transformations. The process is repeated until the cost function asymptotically converges to give the best fit of the TDM.

The theoretically expected mode is calculated from the properties of our experimental setup. The primary element determining the mode of the heralded photon is the narrowband filter cavity C2 in the idler channel. Additionally, the mode's bandwidth is limited by the ~ 50 MHz gain bandwidth of the four-wave mixing process used to generate the biphotons. This effect is taken into account in theoretical plots in Figs. 2 and 3, however we neglect it in the theoretical expressions below for clarity.

The Lorentzian filter C2 in the idler channel produces a signal photon with the TMF in the shape of a *rising* exponential that terminates at the trigger event [22]:

$$\phi(t) = \sqrt{\gamma} e^{\gamma t/2} \Theta(-t), \quad (7)$$

where $\Theta(t)$ is the Heaviside step function and $\gamma = 2\pi \times 7$ MHz is the narrowband cavity linewidth. This exponentially rising mode is of particular significance for applications such as high-efficiency excitation of an atom [23, 24] or a resonator [25, 26] with a single photon. To our knowledge, this is the first demonstration of complete reconstruction of this mode.

Results and Discussion

Fig. 3(a) shows the TDM obtained by iterative reconstruction from the experimental data along with the theoretical predictions. The primary eigenvector of the TDM has a corresponding eigenvalue almost 45 times larger than the second largest one indicating a nearly pure temporal mode. The TDM is primarily real and matches well

the theoretical prediction.

Next, we demonstrate the reconstruction of a temporal mode with a nonvanishing imaginary component. To this end, we induce a virtual frequency shift by redefining the signal-LO detuning according to $\delta\omega' = \delta\omega + \Delta$ when reconstructing the TDM from Eq. (6). The theoretically expected TMF and TDM then become:

$$\phi_{\Delta}(t) = \phi(t)e^{i\Delta t}; \quad (8)$$

$$\rho_{\Delta}(t, t') = \rho(t, t')e^{i\Delta(t-t')}. \quad (9)$$

The TDM reconstructed from the experimental data using the effective modulation frequency of $\Delta = 2\pi \times 5$ MHz is shown in Fig. 3(b). While the purity of the temporal mode is maintained, the reconstructed density matrix now has a significant imaginary component, demonstrating the ability of our technique to accurately reconstruct states with complex temporal modes.

This example is practically relevant in a situation when one does not know the frequency of the photon precisely. In this case, heterodyne measurements at different LO detunings relative to a given reference (defined by the point $\delta\omega = 0$) will provide full information about the mode, including the spectral offset of the photon with respect to that reference.

Finally, we illustrate the ability of our experimental technique to reconstruct the TDM in the case of a mixed state. We phase modulate the signal photons at a frequency $\omega_m = 2\pi \times 20$ MHz, larger than the spectral width of C2. This is achieved by passing the idler photons through an electro-optic modulator (EOM), with its optical axis oriented along the photon's polarization [27]. This leads to a TMF $\phi^{\text{EOM}}(t, \theta_m) = \sqrt{\gamma}e^{\gamma t/2}e^{i\beta \sin(\omega_m t + \theta_m)}\Theta(-t)$, where $\beta = 1.1$ is the modulation index and θ_m is the phase of the modulating voltage at the time when the idler photon is detected. Because the idler photon detections occur at random times, θ_m is randomized, leading to the following non-pure TDM:

$$\begin{aligned} \rho_{t,t'}^{\text{EOM}} &= \frac{1}{2\pi} \int_{-\pi}^{\pi} \phi^{\text{EOM}}(t, \theta_m) [\phi^{\text{EOM}}(t', \theta_m)]^* d\theta_m \quad (10) \\ &= \gamma e^{\frac{\gamma(t+t')}{2}} \Theta(-t)\Theta(-t') J_0 \left[2\beta \sin \left(\frac{\omega_m(t-t')}{2} \right) \right], \end{aligned}$$

where J_0 is the Bessel function of the first kind.

The experimentally reconstructed TDM is shown in Fig. 3(c). The mixed nature of the density matrix is evident from the distribution of eigenvalues, with the ratio of the first and second eigenvalues being only around 2. Due to the modulation phase randomization, the imaginary part of the density matrix is zero.

The observed artifacts in the reconstructed photon modes can be attributed to the finite bandwidth, or non-instantaneous response, of the homodyne detector. This results in the smearing of the acquired autocorrelation matrix. This effect is particularly significant where

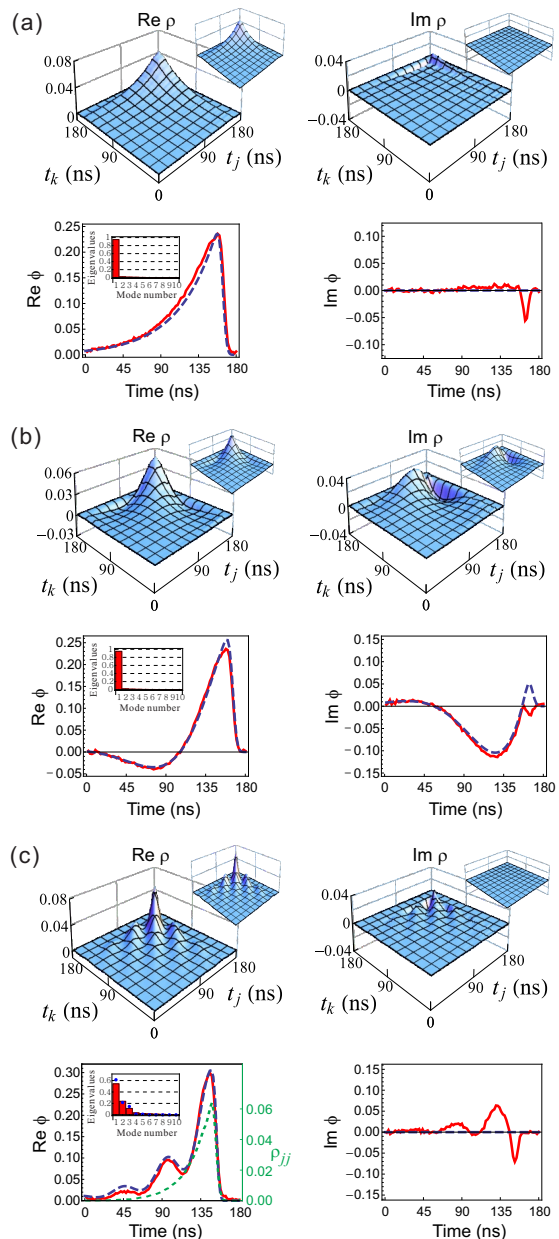


FIG. 3. Experimentally reconstructed temporal modes and their theoretical predictions for the cases without modulation (a), with virtual phase modulation (b), and with phase-randomized EOM modulation (c). For each case, the top two panels show the real (left) and imaginary (right) parts of the TDM, with the insets showing corresponding theoretical plots. Lower two panels show the TDM's primary eigenvector as reconstructed from experimental data (solid red) and theoretical modeling (dashed blue). The green dotted line in (c) also shows the diagonal of the TDM, which is not affected by the modulation as expected from Eq. (10). The insets in the lower left panels show the distribution of eigenvalues (red bars) obtained experimentally. Without EOM modulation (a, b), the theoretically expected mode is pure so the TDM is expected to have only one nonvanishing eigenvector. In the case with EOM modulation (c), the TDM is mixed and the solid blue dots in the inset show theoretical eigenvalues. The trigger photon arrives at $t = 155$ ns for (a), (b) and at $t = 145$ ns for (c).

this matrix has sharp features, such as the trigger event where the photon pulse instantly terminates according to Eq. 7, as seen in Fig. 3(a,b). The fast modulation of the TMF such as in Fig. 3(c) has a similar effect on the reconstructed mode over its entire duration, resulting in a spurious nonzero imaginary part. The observed artifacts, however, do not significantly degrade the fidelities of the experimentally obtained TDMs with respect to the theoretically expected ones. These fidelities, defined as $F = \text{Tr}[\sqrt{\sqrt{\rho_{\text{exp}}}\rho_{\text{th}}\sqrt{\rho_{\text{exp}}}}$ with the subscripts indicating theory versus experiment, are found to be 0.97, 0.94 and 0.93, respectively, for the three cases of Fig. 3.

Using the absolute value of the TMF obtained for the primary mode of the unmodulated case [Fig. 3(a)], we reconstruct the quantum state of light in that mode in the Fock basis akin to Ref. [16], obtaining the single-photon efficiency of $\rho_{11} = 52.9\%$. The corresponding Wigner function, exhibiting negative values at the phase-space origin, is plotted in Fig. 1(c) along with the acquired quadrature distribution and the reconstructed density matrix.

Summary

We have developed and experimentally demonstrated polychromatic optical heterodyne tomography, a robust method for complete experimental determination of the temporal properties of a single photon directly from the time-resolved photocurrent statistics of a balanced homodyne measurement. The method enables the extraction of a temporal mode which in general may be complex and can have multiple frequency components. Accurate detection of the temporal mode is key for the proper mode matching required by many quantum communication protocols.

Our method permits straightforward extension to states other than the single-photon Fock state akin to Ref. [17] provided that the state in question occupies a well-defined spatiotemporal mode. On the other hand, the single-photon state is special in that it can be directly associated with the photon annihilation operator of a certain optical mode or a mixture thereof. The problem of defining the optical mode(s) for a general quantum optical state is a subject of a separate study.

Although the technique described in this work requires the frequency spectrum of the photon's temporal mode to be sufficiently narrowband so its temporal structure can be resolved by the homodyne detector, one can envision ways to lift this restriction. For example, if the photon is produced in an ultrashort pulsed mode, one can extend it in time using a dispersive element such as an optical fiber, and perform time-resolved homodyne detection using a matched chirped local oscillator. The time-domain correlations of the homodyne photocurrent will then correspond to quantum coherences between components of the photon spectrum.

Acknowledgements

ZQ and ASP contributed equally to this work. We thank Erhan Saglamyurek and Wolfgang Tittel for lending us the EOM. The project is supported by NSERC and CIFAR. AL is a CIFAR Fellow. ZQ is supported by the China Scholarship Council.

* LVOV@ucalgary.ca

- [1] Gisin, N., Ribordy, G., Tittel, W. & Zbinden, H. Quantum cryptography. *Rev. Mod. Phys.* **74**, 145–195 (2002).
- [2] Bouwmeester, D., Pan, Jian-Wei., Mattle, K., Eibl, M., Weinfurter, H. & Zeilinger, A. Experimental quantum teleportation. *Nature* **390**, 575–579 (1997).
- [3] Duan, L.-M., Lukin, M. D., Cirac, J. I. & Zoller, P. Long-distance quantum communication with atomic ensembles and linear optics. *Nature* **414**, 413–418 (2001).
- [4] Knill, E., Laflamme, R., & Milburn, G. J. A scheme for efficient quantum computation with linear optics. *Nature* **409**, 46–52 (2001).
- [5] Grosshans, F. & Grangier, P. Effective quantum efficiency in the pulsed homodyne detection of a n-photon state. *Eur. Phys. J. D* **14**, 119–125 (2001).
- [6] Aichele, T., Lvovsky, A. I., & Schiller, S. Optical mode characterization of single photons prepared by means of conditional measurements on a biphoton state. *Eur. Phys. J. D* **18**, 237–245 (2002).
- [7] Keller, M., Lange, B., Hayasaka, K., Lange, W., & Walther, H. Continuous generation of single photons with controlled waveform in an ion-trap cavity system. *Nature* **431**, 1075–1078 (2004).
- [8] Mølmer, K. Non-Gaussian states from continuous-wave Gaussian light sources. *Phys. Rev. A* **73**, 063804 (2006).
- [9] Sasaki, M. & Suzuki, S. Multimode theory of measurement-induced non-Gaussian operation on wideband squeezed light: Analytical formula. *Phys. Rev. A* **73**, 043807 (2006).
- [10] Lvovsky, A. I. & Raymer, M. G. Continuous-variable optical quantum-state tomography. *Rev. Mod. Phys.* **81**, 299 (2009).
- [11] Lundeen, J. S., Sutherland, B., Patel, A., Stewart, C. & Bamber, C. Direct measurement of the quantum wavefunction. *Nature* **474**, 188–191 (2011).
- [12] Polyakov, S. V., Chou, C. W., Felinto, D. & Kimble, H. J. Temporal dynamics of photon pairs generated by an atomic ensemble. *Phys. Rev. Lett.* **93**, 263601 (2004).
- [13] Flagg, E. B., Polyakov, S. V., Thomay, T. & Solomon, G. S. Dynamics of nonclassical light from a single solid-state quantum emitter. *Phys. Rev. Lett.* **109**, 163601 (2012).
- [14] Polycarpou, C., Cassemiro, K. N., Venturi, G., Zavatta, A. & Bellini, M. Adaptive detection of arbitrarily shaped ultrashort quantum light states. *Phys. Rev. Lett.* **109**, 053602 (2012).
- [15] MacRae, A. An Atomic Source of Quantum Light. Ph.D. thesis, University of Calgary (2012).
- [16] MacRae, A., Brannan, T., Achal, R. & Lvovsky, A. I. Tomography of a high-purity narrowband photon from a transient atomic collective excitation. *Phys. Rev. Lett.* **109**, 033601 (2012).
- [17] Morin, O., Fabre, C. & Laurat, J. Experimentally access-

ing the optimal temporal mode of traveling quantum light states. Phys. Rev. Lett. **111**, 213602 (2013).

- [18] Although single photons associated with a certain moment in time are ill-defined, treatment (1) is approximately valid as long as the spectral width of the photon is much less than its frequency. See M.V. Fedorov *et al.*, Phys. Rev. A **72**, 032110 (2005) for a detailed discussion of this matter.
- [19] Palittapongarnpim, P., MacRae, A. & Lvovsky, A. I. Note: A monolithic filter cavity for experiments in quantum optics. Rev. Sci. Instrum. **83**, 066101 (2012).
- [20] Kumar, R., Barrios, E., MacRae, A., Cairns, E., Huntington, E. H. & Lvovsky, A. I. Versatile wideband balanced detector for quantum optical homodyne tomography. Opt. Comm. **285**, 5259–5267 (2012).
- [21] Appel, J., MacRae, A. & Lvovsky, A. I. A versatile digital GHz phase lock for external cavity diode lasers. Meas. Sci. Technol. **20**, 055302 (2009).
- [22] See supplementary information.
- [23] Aljunid, S. A., Maslennikov, G., Wang, Y., Dao, H., Scarani, V. & Kurtsiefer, C. Excitation of a Single Atom with Exponentially Rising Light Pulses. Phys. Rev. Lett. **111**, 103001 (2013).
- [24] Gulati, G. K., Srivathsan, B., Chng, B., Cerè, A., Matsukevich, D. & Kurtsiefer, C. Counterintuitive temporal shape of single photons. arXiv:1402.5800 (2014).
- [25] Bader, M., Heugel, S., Chekhov, A. L., Sondermann, M. & Leuchs, G. Efficient coupling to an optical resonator by exploiting time-reversal symmetry. New J. Phys. **15**, 123008 (2013).
- [26] Liu, C., Sun, Y., Zhao, L., Zhang, S., Loy, M. M. T. & Du, S. Efficiently loading a single photon into a single-sided Fabry-Perot cavity. Phys. Rev. Lett. **113**, 133601 (2014).
- [27] Kolchin, P., Belthangady, C., Du, S., Yin, G. Y. & Harris, S. E. Electro-optic modulation of single photons. Phys. Rev. Lett. **101**, 103601 (2008).

APPENDIX

Derivation of temporal wavefunction

The theoretical TMF for the single photon can be obtained as follows. The biphoton generated by the four-wave mixing process with an infinite gain bandwidth can be represented as

$$|\Psi\rangle = \int |1_{\omega_s}, 1_{\omega_i}\rangle \delta(\omega_s + \omega_i - 2\omega_p) d\omega_s d\omega_i \quad (11)$$

where indices s , i and p correspond to signal, idler and pump respectively. The amplitude transmission function of the cavity in the neighborhood of its resonance can be expressed as a function of the detuning of the beam from the cavity resonance frequency $\delta_i = \omega_c - \omega_i$ as $T(\delta_i) = \sqrt{2/\pi\gamma}(1 - 2i\delta_i/\gamma)^{-1}$, where γ is the linewidth of the cavity. Subjecting the idler channel to transmission

through this cavity, state (11) transforms into:

$$|\Psi'\rangle = \sqrt{\frac{2}{\pi\gamma}} \int \frac{1}{1 - 2i\frac{\delta_i}{\gamma}} \delta(\omega_s + \omega_i - 2\omega_p) |1_{\omega_s}, 1_{\omega_i}\rangle d\omega_s d\omega_i. \quad (12)$$

Subsequent idler photon detection at time t_i will project the signal onto the state $|\tilde{\phi}_s\rangle = \langle 1_{t_i} | \Psi'\rangle$ where $|1_{t_i}\rangle = \int |1_{\omega_i}\rangle e^{i\delta_i t_i} d\omega_i$. Assuming that the detection event happens at $t_i = 0$, the resultant state in the signal channel in the frequency domain can be expressed as

$$|1_{\phi_s}\rangle = \langle 1_{t_i=0} | \Psi'\rangle = \sqrt{\frac{2}{\pi\gamma}} \int \frac{1}{1 + 2i\frac{\delta_s}{\gamma}} |1_{\omega_s}\rangle d\omega_s, \quad (13)$$

where $\delta_s = 2\omega_p - \omega_c - \omega_s$ is the detuning of the signal frequency from the central frequency determined by the cavity. Performing a Fourier transform on Eq. (13), we find the temporal mode of the signal photon:

$$|1_{\phi_s}\rangle = \sqrt{\gamma} \int e^{\gamma t_s/2} \Theta(-t_s) |1_{t_s}\rangle dt_s \quad (14)$$

where $\Theta(\cdot)$ is the step function.

Ambiguity of reconstruction with a single LO frequency

If only a single LO frequency with $\delta\omega = 0$ were used, as in Refs. [1, 2], mode reconstruction would only yield a real part of the TDM. To present direct evidence of incompleteness of such reconstruction, we specialized to the situation of Fig. 3(b) (virtual phase modulation) and acquired the homodyne photocurrent autocorrelation for the photon detuned from the local oscillator by $\Delta = \pm 10.8$ MHz (Fig. S1). The TDMs corresponding to these situations are complex conjugate of each other: $\rho_{\Delta}(t, t') = \gamma e^{\gamma(t+t')/2} \Theta(-t) \Theta(-t') e^{\pm i\Delta(t-t')}$. However, the reduced autocorrelation matrix $\text{Re}\rho_{\Delta}(t, t')$ is the same in both these cases or for their arbitrary statistical mixture.

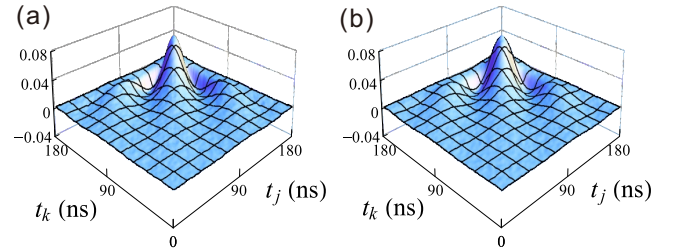


FIG. S1. Experimentally observed reduced autocorrelation matrices $\text{Re}\rho_{\Delta}(t, t')$ for $\Delta = 10.8$ MHz (a) and $\Delta = -10.8$ MHz (b). These matrices are identical, although the temporal modes are different.

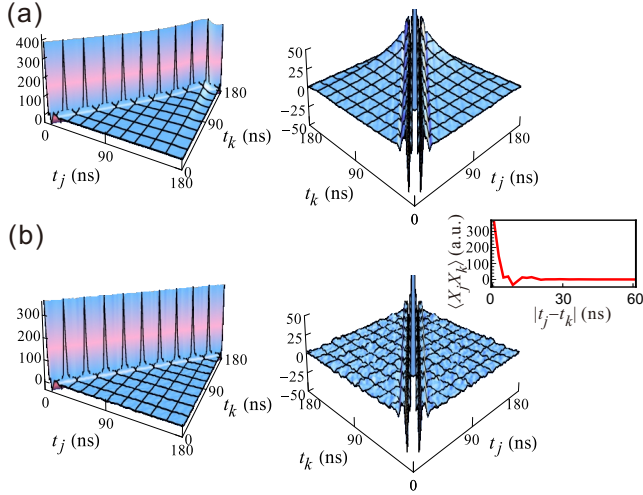


FIG. S2. Experimentally observed autocorrelation matrices of the homodyne detector photocurrent for (a) the single-photon signal with zero LO detuning, no modulation and (b) vacuum signal. Two different viewpoints and plot ranges are used for better visibility. The reduced autocorrelation matrix [Fig. 2(b) of the main text] is obtained by subtracting (b) from (a). The inset shows the mean homodyne detector photocurrent autocorrelation $\langle X_j X_k \rangle$ for the vacuum case as a function of $|t_j - t_k|$. The vertical axis scale is arbitrary.

Calculating reduced autocorrelation matrices

The experimentally obtained full autocorrelation matrices are shown in Fig. S2 for the signal being in the single-photon (a) and vacuum (b) states. These matrices are described by Eqs. (5) and (6) in the main text. The matrix in (a) contains both terms of Eq. (5), while that of (b) only the first term. One can see that the first term is dominant, while the “payload” second term emerges only as a small feature in Fig. S2(a). This is to be expected: according to Eq. (5), the magnitude of the first term is $1/2$ whereas that of the second term is determined by the typical TDM element, which is the inverse duration of the photon’s temporal mode measured in digitizer time bins (because the trace of the density matrix must be one). As seen from Fig. 3 in the main text, the largest elements of the normalized density matrix do not exceed 0.06–0.07. Note that using excessive

temporal resolution of the digitizer is therefore not advisable, as it will reduce the ratio between that density matrix and the vacuum term.

Additionally, the experimental autocorrelation matrices are affected by the statistical uncertainties. For each waveform sample and a specific pair of time bins, the variance of the autocorrelation is evaluated for the vacuum case as

$$\langle \Delta(X_j X_k)^2 \rangle = \langle X_j^2 \rangle \langle X_k^2 \rangle = \frac{1}{4}.$$

For N waveforms acquired, the standard deviation of the mean autocorrelation value is therefore $1/(2\sqrt{N})$. For the single-photon case, the statistical noise is of the same magnitude. For reliable reconstruction of the mode, this noise must be much less than the typical density matrix element. We address this issue by acquiring large quantities of data samples: $N = 2 \times 10^6$ waveforms for each LO frequency. This is much more than the number of samples collected in a typical quantum state tomography experiment.

In practice, both terms of Eq. (5), as well as the statistical fluctuations, are smeared by the non-instantaneous response of the detector (Fig. S2). Fortunately, this smearing primarily affects the undesired first term and the fluctuations because of their singular nature.

A full set of reduced autocorrelation matrices

Eight normalized reduced autocorrelation matrices for the case without modulation are presented in Fig. S3, and the theoretically calculated reduced autocorrelation matrices are also shown for comparison.

* LVOV@ucalgary.ca

- [1] MacRae, A., Brannan, T., Achal, R. & Lvovsky, A. I. Tomography of a high-purity narrowband photon from a transient atomic collective excitation. *Phys. Rev. Lett.* **109**, 033601 (2012).
- [2] Morin, O., Fabre, C. & Laurat, J. Experimentally accessing the optimal temporal mode of traveling quantum light states. *Phys. Rev. Lett.* **111**, 213602 (2013).

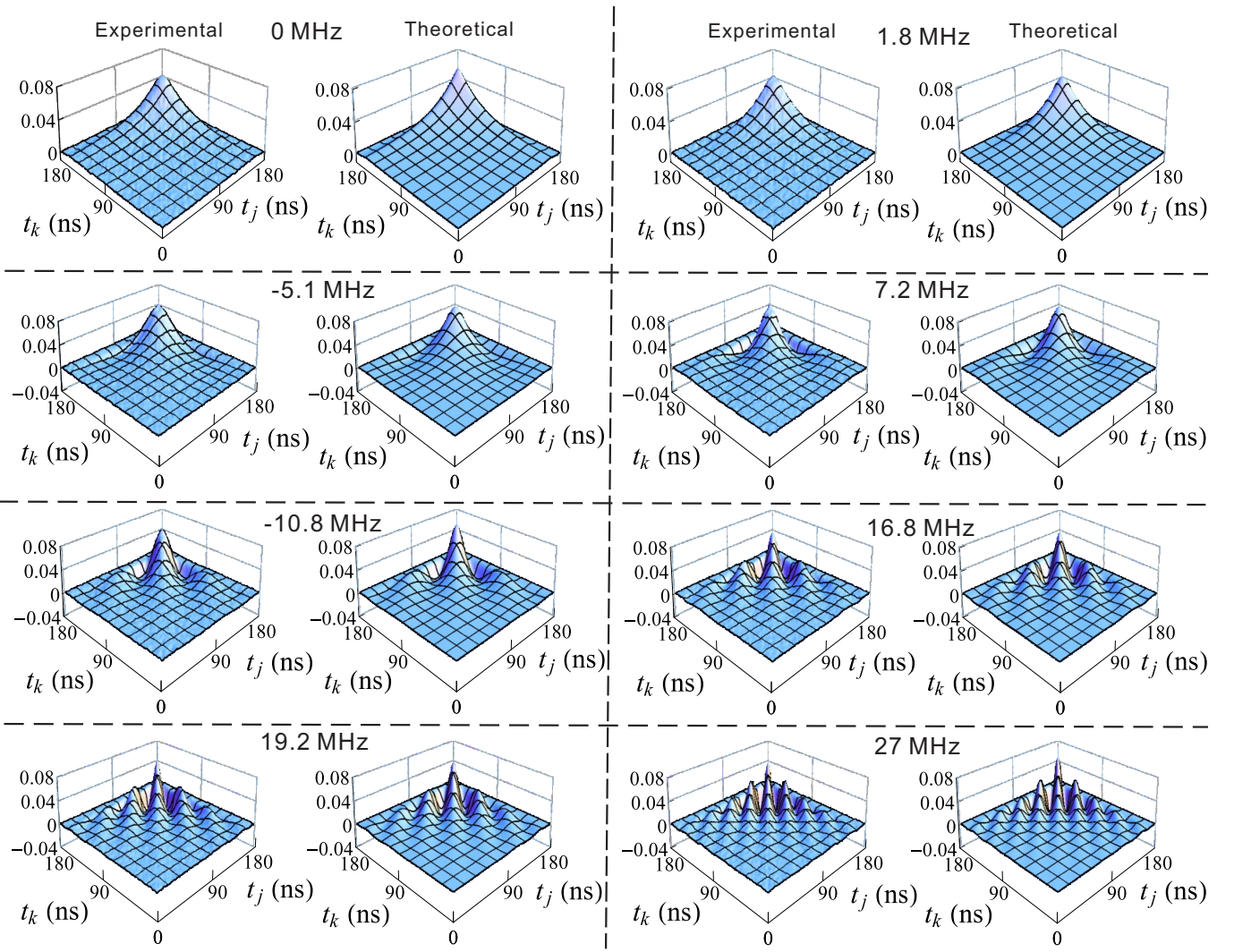


FIG. S3. Theoretical (right) and experimental (left) reduced autocorrelation matrices, for eight different LO detunings, corresponding to the measurement setting without modulation. The trigger photon arrives at $t = 155$ ns.